Zeitschrift für Physikalische Chemie, Bd. 201, S. 21–30 (1997)

Isotope Shift of Local Vibrational Modes at Transition-Metal Impurities in Semiconductors*

By C. Schrepel, C. Göbel, U. Scherz

Institut für Theoretische Physik, Technische Universität Berlin

P. Thurian, G. Kaczmarczyk and A. Hoffmann

Institut für Festkörperphysik, Technische Universität Berlin, Hardenbergstr. 36, D-10623 Berlin, Germany

(Received August 25, 1996)

Jahn-Teller effect / Isotope effect / Local vibrational modes / Impurity / ZnS, ZnO

The observation of isotope effects in the fine structure of optical transitions at transition-metal impurities in II–VI compounds is mainly due to a Jahn-Teller effect. In case of the transitions between the multiplets $^4T_1(F) \leftrightarrow {}^4T_1(P)$ of Ni^{2+} centers in cubic ZnS, the positive isotope shift of various lines with respect to the masses of ^{58}Ni, ^{60}Ni, and ^{64}Ni is due to the coupling to local vibrational modes of T_2 symmetry. The isotope shift of the Raman active modes at 26.2 meV and 38.9 meV are calculated to be $-28.3\ \mu$eV/nucleon and $-25.2\ \mu$eV/nucleon, respectively. These results were obtained by using the valence-force model of Keating and Kane together with the long-range Coulomb forces and the scaling-factor approximation. The fine-structure transitions between the multiplets $^2T_2 \leftrightarrow {}^2E$ of Cu^{2+} centers in hexagonal ZnO show negative isotope effects with respect to the masses of ^{65}Cu and ^{63}Cu and in addition isotope effects with respect to the ligands of the impurity ^{16}O and ^{18}O. We point out that these isotope shifts are due to the Jahn-Teller coupling of a local vibrational mode (LVM) of $T_2 = A_1 \times E$ symmetry in the $^2T_2$ multiplet and that the anisotropic vibration of the four O ligands of this LVM explains the difference in the $^{16/18}O$ isotope shift where the c axis ^{16}O and one of the off axis ^{16}O is replaced by ^{18}O respectively.

I. Introduction

The optical spectra of transition-metal impurities in II–VI compounds, originating from internal transitions between energy levels of 3d electrons,

* Presented at the 13th International Symposium on Electrons and Vibrations in Solids and Finite Systems (Jahn-Teller Effect) Berlin 1996.

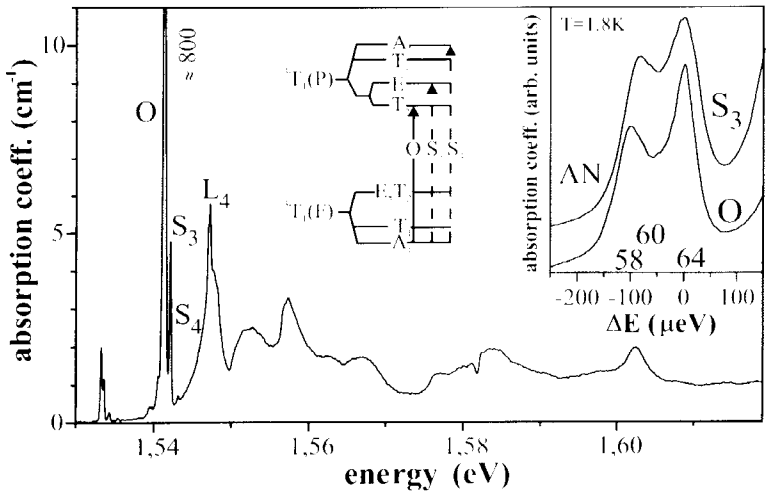

Fig. 1. Absorption spectrum of Ni^{2+} centers in cubic ZnS crystals at T = 1.8 K. The isotope splitting of the two main zero phonon lines O and S_3 is shown in the insert.

are determined by crystal-field splitting and electron-phonon interaction. This can be seen from the phonon sidebands of the zero-phonon lines and from a quantitative interpretation of the observed fine-structure lines in terms of a dynamical Jahn-Teller effect. The observation of an isotope effect indicates the coupling of the electronic transition to at least one local vibrational mode (LVM) [1]. In most cases it is possible to understand the optical fine structure and the magnetic field splitting by coupling to a single or two LVMs if a sufficient number of excited vibrational energy levels are taken into account [2]. Such LVMs, localized at the defect site, are also observed by Raman spectroscopy, which yields the phonon energy and symmetry. In order to understand the isotope shift of a particular optical fine-structure transition it is necessary to calculate the dependence of the energy of the LVM on the impurity or ligand mass and the shift of the energy levels of the initial and final vibronic state from a variation of the energy of the LVM [3]. We here present measurements of different isotope effects observed for zero-phonon lines (ZPLs) of intercenter $d-d$ transitions and investigate the isotope shift of the LVMs only, whereas the second step is a result of the fine-structure fitting procedure to the various crystal-field parameters and the Jahn-Teller energy. It is, however, often not clear which LVMs are involved in the fine-structure energy level scheme [4] and only some of them may cause the isotope effect.

In Section II we discuss the observed isotope effects and in Section III the model of the LVMs and their dependence of the atomic masses. In

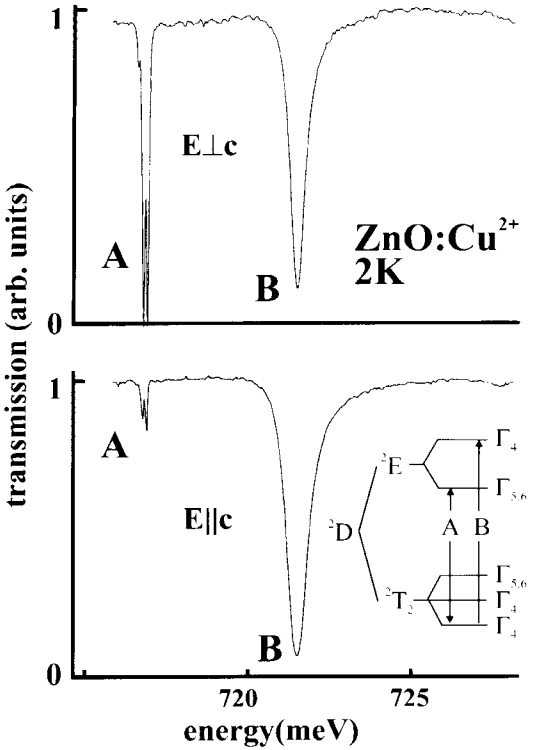

Fig. 2. Transmission spectrum of Cu^{2+} centers in hexagonal ZnO crystals at $T = 2$ K for a polarization of the electric field vector parallel and perpendicular to the c axis, respectively. The insert shows the transitions A and B from the $^2T_2$ ground state to the ^2E excited state.

Section IV we present the results for Ni impurities in cubic ZnS crystals and in Section V for the impurity and ligand isotope effect for Cu impurities in hexagonal ZnO crystals.

II. Experimental results

The optical absorption spectrum in the near infrared region of the $^3T_1(F) \rightarrow {}^3T_1(P)$ transition of Ni^{2+} centers in cubic ZnS at $T = 1.8$ K is shown in Fig. 1, see Ref. [5] for the details. The insert shows the assignments of the main zero-phonon lines to the transitions between the two multiplets. The isotope splitting of the zero-phonon lines O and S_3 was measured with a magnetic field parallel to the [111] axis and is also shown

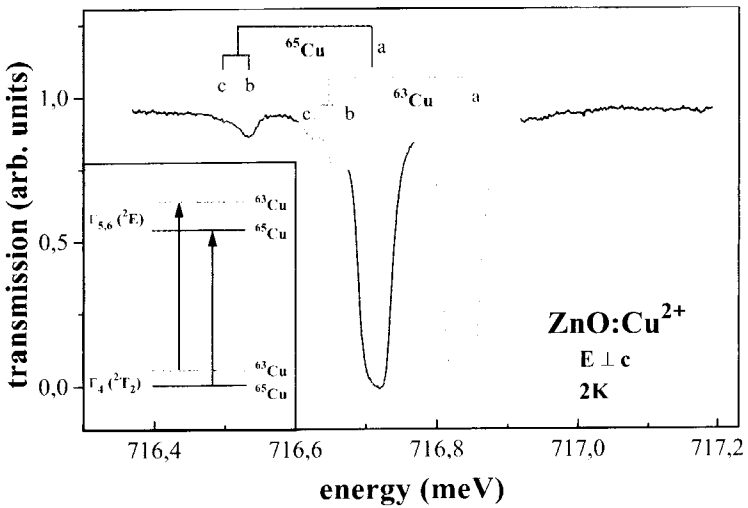

Fig. 3. Polarized transmission spectrum showing the isotope shifts of the Cu^{2+} absorption line *A* in ZnO at $T = 2$ K. The main lines are due to the impurity induced isotope effect and the smaller lines are due to the ligand induced isotope effect.

in the other insert. The result is 17.0 μeV/nucleon for the *O* line and 14.3 μeV/nucleon for the S_3 line. There is also a richly structured sideband on the high-energy side of the dominating *O* line.

The transmission spectrum of the Cu^{2+} absorption in ZnO crystals is shown in Fig. 2, see Ref. [6] for the details. The isotope splitting of the zero-phonon line *A* of Fig. 2 is shown in Fig. 3 in case of the polarization of the electric field vector perpendicular to the *c* axis [7]. The main splitting of the *A* line is attributed to the two copper isotopes ^{65}Cu and ^{63}Cu and both lines have two satellites, which are attributed to transitions where one of the four ^{16}O ligands is substituted by an ^{18}O isotope. The two lines of this ligand induced isotope effect originate from the difference between the substituted ^{18}O atom in a position on the *c* axis with respect to the impurity site and a position off the *c* axis. The impurity induced isotope shift is -61 μeV/nucleon and the ligand induced isotope shift is -90 μeV/nucleon for an ^{18}O off the *c* axis and -102 μeV/nucleon for an ^{18}O on the *c* axis.

III. Model for local vibrational modes

The isotope shift of a fine-structure transition results from different isotope shifts of the energy levels of the initial and final vibronic states. These energy levels depend on various crystal-field parameters, the Jahn-Teller energy and the energies of the LVMs involved. Only strongly localized

modes can cause an isotope shift of a vibronic energy level as a result of a different impurity or ligand atomic mass. The change of the energy of the LVM with the mass of one atom of the defect depends on the localization of the LVM or, more precisely, on the vibration amplitude of that particular atom.

In order to calculate the mass dependence of a LVM we used the valence-force model (VFM) of Keating [8] and Kane [9] together with the long-range Coulomb forces to describe the interatomic forces in terms of four valence-force parameters and an effective charge of the vibrating atoms. The dynamical matrix is then set up and diagonalized numerically as a function of these parameters. The eigenvalues of the dynamical matrix are the squares of the vibration frequencies. The valence-force parameters of the perfect crystal are then determined by fitting the phonon energies to the experimental phonon dispersion curves. The valence-force parameters, describing the interatomic forces in the vicinity of the defect, are taken using the scaling-factor approximation (SFA). This approximation assumes an equal relative change of all forces at the defect with respect to the perfect crystal values. We use a cluster of several hundred vibrating atoms around the impurity, which is embedded in a non-vibrating crystal. The eigenvalues of the dynamical matrix of such a cluster give us the vibration frequencies and the eigenvectors describe the relative vibration amplitudes of the various atoms. We select the LVMs from their strong localization or large vibration amplitudes of the atoms in the vicinity of the defect. The scaling factor is then obtained from the fitting of the energy of the LVMs to observed Raman modes. This approximation can well describe the isotope effect observed at various LVMs [10].

Irrespective of the validity of a VFM there exists a simple way to calculate the derivative of the energy $\hbar\omega$ of a LVM with respect to the mass M of a particular atom. Let A^2 be the sum of the squares of the three corresponding components of the eigenvector of the dynamical matrix, then $A/\sqrt{M}$ is the relative vibration amplitude of that atom and we have

$$\frac{M}{\hbar\omega}\frac{d\hbar\omega}{dM} = -\frac{1}{2}A^2 \quad \text{with} \quad 0 \leq A^2 \leq 1. \tag{1}$$

This equation allows the determination of the shift of the energy of a LVM with respect to different impurity or ligand isotopes from the corresponding eigenvector of the dynamical matrix.

IV. Local vibrational modes at ZnS:Ni

The valence-force parameters of Keating and Kane for the perfect cubic ZnS crystal were obtained from fitting to experimental phonon dispersion curves [11], and the resulting density of phonon states is shown in Fig. 4.

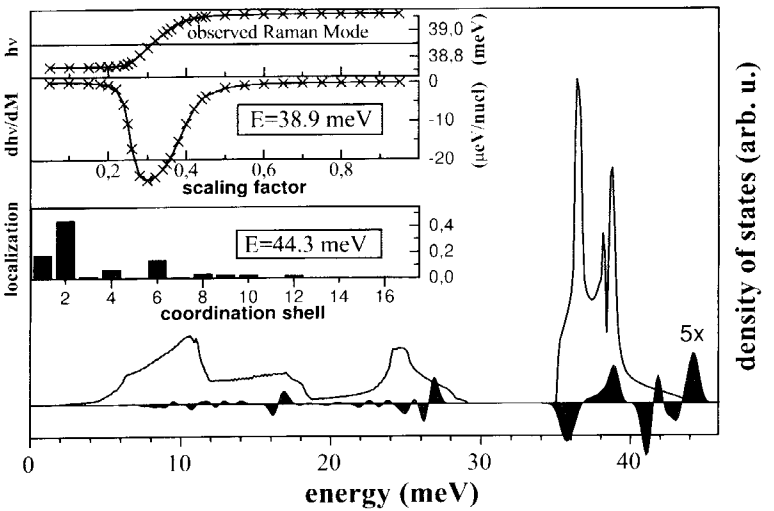

Fig. 4. Density of phonon states of a perfect cubic ZnS crystal together with the change of the density of phonon states as a result of a Ni impurity. The strong localization of the LVM at 44.3 meV is shown in the lowest insert. The other inserts show the change of the energy and of the mass derivative of the energy of the LVM with the change of the scaling factor.

The figure also shows the change of the density of phonon states due to the Ni impurity. This was calculated with a cluster of 281 vibrating atoms with a scaling factor of 0.3. The localization of a strongly localized LVM at 44.3 meV is visualized in the lowest insert. Here the number indicate the various coordination shells of atoms having the same distance from the impurity site. The bars give the relative vibration amplitudes summed up for all atoms of one coordination shell, as obtained from the eigenvectors of the dynamical matrix. The highest insert shows the energy of the LVM at 38.9 meV as a function of the scaling factor. It can be seen that the LVM coincides with the observed Raman mode at 38.9 meV at a scaling factor close to 0.3. The change of localization of the LVM with the scaling factor is demonstrated from the derivative of the energy $\hbar\omega$ of the LVM with the mass M of the Ni impurity, which is shown in the middle of the three inserts. The change of the mass derivative is due to the change of hybridization of the LVM with crystal phonons. The application of Eq. (1) then gives $d\hbar\omega_1/dM = -25.3\,\mu$eV/nucleon for the LVM at $\hbar\omega_1 = 38.8$ meV and $d\hbar\omega_2/dM = -28.3\,\mu$eV/nucleon for the LVM at $\hbar\omega_2 = 26.2$ meV.

V. Local vibrational modes at ZnO:Cu

The valence-force parameters of Keating and Kane for the perfect hexagonal ZnO crystal were obtained from fitting to experimental phonon dis-

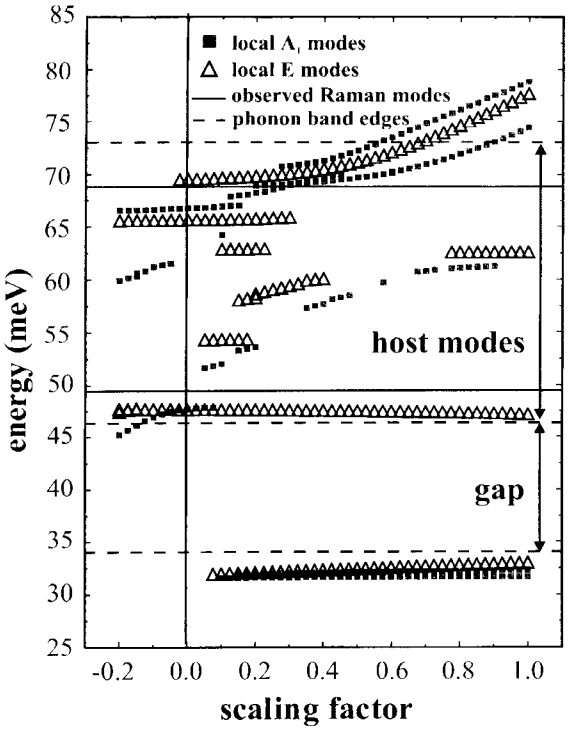

Fig. 5. Energy of LVMs in ZnO:Cu with more than 30% localization on the impurity and its 26 neighbours as a function of the scaling factor.

persion curves [12], and the resulting density of phonon states is shown in the insert of Fig. 6. Fig. 5 shows the energy of the LVMs with more than 30% localization on the impurity and its 26 neighbours as a function of the scaling factor. Except for two close LVMs with E and A_1 symmetry, which are due to the splitting of a cubic T_2 mode, all LVMs are localized a few per cent on the impurity only for the range of the scaling factor considered and therefore cannot cause the $^{63/65}$Cu isotope shift. This is specially true for the observed Raman modes [13] at $\hbar\omega = 49.47$ meV and $\hbar\omega = 68.83$ meV. For the LVM of A_1 symmetry and the LVM of E symmetry at $\hbar\omega \approx 32.0$ meV the relative vibration amplitude of the impurity increases almost linearly from 2.8% at a scaling factor 0.0 up to 12.4% at a scaling factor 1.0 and from 5% up to 18% respectively. The localization of these LVMs at the scaling factor 0.5 is visualized in Fig. 6. Here the numbers indicate the various coordination shells of atoms having the same distance from the impurity site. The impurity (Cu) is denoted by one, the four nearest neighbour atoms (O) are denoted by two, the second nearest neighbours

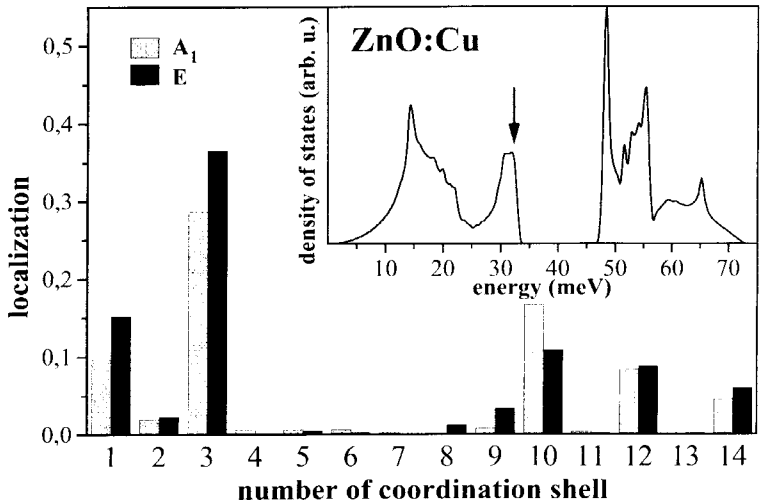

Fig. 6. The localization of the LVMs of A_1 and E symmetry at $\hbar\omega \approx 32$ meV at the scaling factor 0.5 in ZnO:Cu. The numbers indicate the various coordination shells of atoms having the same distance from the impurity site. The bars give the localization summed up for all atoms of one coordination shell. The insert shows the calculated density of phonon states of the perfect hexagonal ZnO crystal.

(Zn) by three and so on. The atoms in shell number 15 and farther atoms are kept at rest. The bars give the localization summed up for all atoms of one coordination shell, as obtained from the eigenvectors of the dynamical matrix. Then the localization of the cubic LVM of T_2 symmetry is the sum of the corresponding localizations of the LVMs of A_1 and E symmetry. It is an interesting fact that for this LVM the contribution of the three off axis O ligands (1.05% per atom) and the contribution of the on axis O ligand (1.13%) to the localization 4.28% of the second coordination shell is different. From these data and the experimental results we conclude that the $^2T_2$ ground state multiplet couples to this cubic T_2 LVM at 32 meV whereas the excited state multiplet ^2E which can not couple to T_2 modes in first order approximation are assumed to show no Jahn-Teller effect. With this model the sign of the $^{63/65}Cu$ as well as the ligand induced isotope shift can be understood. The difference in the observed $^{16/18}O$ isotope shift where the c axis ^{16}O and one of the off axis ^{16}O is replaced by ^{18}O respectively, is then a consequence of the anisotropic vibration of the four O ligands of this LVM.

VI. Discussion

According to our model the zero phonon state $\Gamma_{5,6} - {}^2E$ of $ZnO:Cu^{2+}$, which is the final state for the absorption line A, has a mass dependence of

1.5 $d\hbar\omega/dM$. For the initial state $\Gamma_4 - {}^2T_2$ the observed $^{63/65}$Cu isotope shift requires a reduction of the 1.5 $d\hbar\omega/dM$ zero phonon value to 0.54 $d\hbar\omega/dM$ at the scaling factor 0.5. Then the resulting ligand induced isotope shifts are $-10\,(-90)\,\mu$eV/nucleon for an off axis oxygen and $-11\,(-102)\,\mu$eV/nucleon for an on axis oxygen. The values in parentheses are the corresponding experimental values. However such a strong reduction of the mass dependence of the vibronic state does not result from a Jahn-Teller effect in case of zero phonon lines. This can be demonstrated for $ZnS:Ni^{2+}$. The fine structure and the Zeeman behaviour of the ${}^3T_1(F) - {}^3T_1(P)$ transition can be explained with a Jahn-Teller coupling of a LVM of T_2 symmetry at $\hbar\omega = 28.7$ meV to the multiplets ${}^3T_1(F)$ and ${}^3T_1(P)$ with Huang-Rhys factors of $S = 0.72$ and $S = 2.41$ respectively [4]. With this model we calculated the mass dependence to 1.299 $d\hbar\omega/dM$ for the $T_2 - {}^3T_1(F)$ state and to 1.151 $d\hbar\omega/dM$ and 1.142 $d\hbar\omega/dM$ for the T_2, $E - {}^3T_1(P)$ states corresponding to a reduction of 15, 31 and 30% from the zero phonon value. The resulting isotope shifts are 4.2 meV and 4.4 meV for the O and S_3 absorption line which had to be compared with 17.0 meV and 14.3 meV respectively.

In summary our model reproduces the sign of the isotope shifts as a consequence of the lower (stronger) Jahn-Teller coupling in the ground state for $ZnS:Ni^{2+}$ ($ZnO:Cu^{2+}$). However the magnitude of the calculated isotope shift is too small in both cases. This may be due to additional Jahn-Teller active LVMs, which contribute to the isotope effect. Specially in $ZnO:Cu^{2+}$ the observed Raman modes at $\hbar\omega = 49.47$ meV and $\hbar\omega = 68.83$ meV are strongly localized to the O ligand and therefore can cause the ligand induced isotope effect. However, for $ZnO:Cu^{2+}$ a possible wrong description of the density of phonon states can cause dramatically change of the localization due to hybridization with the host modes and therefore significantly increase the mass dependence of the LVM.

Acknowledgement

We thank Henrik Siegle for valuable discussions. We thank the Zentraleinrichtung Rechenzentrum of the Technische Universität Berlin for their support and the provision of computing facilities.

References

1. J. Schöpp, R. Heitz, A. Hoffmann and U. Scherz, Mater Sci. Forum **143–147** (1994) 815.
2. T. Telahun, P. Thurian, A. Hoffmann, I. Broser and U. Scherz, Mater. Sci. Forum **196–201** (1995) 767.
3. A. Hoffmann and U. Scherz, J. Cryst. Growth **101** (1990) 385.
4. C. Schrepel, J. Schöpp, R. Heitz, A. Hoffmann and U. Scherz, Mater. Sci. Forum **196–201** (1995) 743.

5. R. Heitz, A. Hoffmann and I. Broser, Phys. Rev. **B50** (1994) 17028.
6. P. Thurian, PhD thesis D83, Technische Universität Berlin (1994).
7. P. Thurian, R. Heitz, S. Kleinwächter, A. Hoffmann and I. Broser, Mater. Sci. Forum **143–147** (1994) 453.
8. P. N. Keating, Phys. Rev. **145** (1966) 637.
9. E. O. Kane, Phys. Rev. **B31** (1985) 7865.
10. U. Scherz and C. Schrepel, Mater. Sci. Forum **196–201** (1995) 1583.
11. N. Vagelatos, D. Wehe and J. S. King, J. Chem. Phys. **60(9)** (1974) 3613.
12. K. Thoma and B. Dorner, Solid State Commun. **15** (1974) 1111.
13. P. Thurian, G. Kaczmarczyk, H. Siegle, R. Heitz, A. Hoffmann, I. Broser, B.-K. Meyer, R. Hoffbauer and U. Scherz, Mater. Sci. Forum **196–201** (1995) 1571.